Stochastic Modeling of Service Life of Concrete Structures in Chloride-Laden Environments

Yajun Liu, Ph.D.[1]; and Xianming Shi, Ph.D., P.E.[2]

Abstract: Chloride-induced rebar corrosion is a common degradation process for concrete infrastructure, which is a practical concern for cold-climate states and coastal areas. In this work, numeric models based on the FEM are utilized to study service life of concrete structures subject to chloride ingress, where two models are utilized. The first one deals with multiple ionic species in the concrete pore solution, while the second one only accounts for the presence of chloride ions. The stochastic nature of model inputs is taken into consideration because each factor of interest is subject to random variabilities and inherent uncertainties. Specifically, the surface chloride concentrations and concrete cover depth follow the normal distribution; the diffusion coefficients obey the gamma distribution; the actual chloride threshold features the triangular distribution. The nonlinear partial differential equations (PDEs) to characterize the spatial and temporal evolution of ionic species are numerically solved, the results of which were utilized to elucidate the influence of various factors on concrete service life, such as mix design, surface chloride concentrations, cracking level, and coarse aggregate and concrete cover depth. **DOI: 10.1061/(ASCE)MT.1943-5533.0000399.**

CE Database subject headings: Finite element method; Service life; Stochastic models; Chloride; Reinforced concrete; Concrete structures.

Author keywords: Finite-element method; Service life prediction; Stochastic modeling; Chloride diffusion; Mineral admixtures; Reinforced concrete.

Introduction

Due to its high strength, flexibility in geometries, and variability in mechanical properties, reinforced concrete has been the most widely used construction materials for infrastructure across the world. Concrete pore solutions can have pH values well above 12, which allows rebar surface to be covered with a thin, passive, and impermeable oxide film (Fasjardo et al. 2002; Orellan et al. 2004). In addition, the dense concrete cover forms a physical barrier to reduce the penetration of deleterious species. Under such protective environments within concrete, steel rebars do not corrode spontaneously, which prevents anodic reactions from occurring and makes steel inert for corrosion.

Chloride-induced degradation in concrete structures is a common occurrence in the United States because of the use of deicers in cold-climate states and the saline environments in coastal areas. By capillary absorption and diffusion, chloride ions can migrate into concrete. Although capillary movement is fast, it is less favored by the discontinuous pore system in concrete. Diffusion thus provides a practical manner for chloride ions to migrate across concrete cover and reach rebar surface, and the transport of chloride ions through concrete cover to rebar surface is a major cause of concrete degradation, the results of which lead to serious economic and safety implications. Chloride ions are responsible for the breakdown of passive film and the initiation of corrosion (Glass and Buenfeld 2000a; Gjrv and Vennesland 1979). Reliable predictions for existing rebar performance are indispensable, which can take into account the extent of deterioration, the expected remaining service life, and optimum repair strategy. A well-defined procedure allows sufficient information to be obtained for timely rehabilitation and replacement of reinforced concrete structures.

Although research of reinforcement corrosion in concrete has been extensively documented in the past decades (Thomas 1996; Glass and Buenfeld 1997, 2000b; Basheer et al. 2001), the current state of knowledge in corrosion initiation remains unsatisfactory. In traditional service life modeling, the concerns are addressed with the stochastic technique, with only the diffusion of chlorides taken into consideration. Such treatments (Khatri and Sirivivatnanon 2004; Konecny et al. 2007) fail to adequately describe concrete degradation resulting from mutual interactions among multiple ionic species, thereby underestimating or overestimating the risk of chloride contamination. In this study, a stochastic model is presented to simulate the service life of concrete structures subject to chloride ingress, the goal of which is to develop a reliable technique to predict structural deterioration and assess the service life of reinforced concrete in typical aggressive environments with the FEM. Within the mathematical framework and the numerical implementation, input parameters are assumed to follow normal, gamma, and triangular distributions, respectively. Such distributions have been frequently employed for stochastic modeling of concrete service life and also verified in real field practice (Tutti 1982; Kirkpatrick et al. 2002, 2003; Jiang et al. 2010). Combined with the chloride binding isotherms, the algorithm of service life

[1]Research Scientist, Corrosion & Sustainable Infrastructure Laboratory, Western Transportation Institute, Montana State Univ., P.O. Box 174250, Bozeman, MT 59717-4250.

[2]Associate Research Professor, Civil Engineering Dept., Montana State Univ., 205 Cobleigh Hall, MT State Univ., Bozeman, MT 59717-3900; Program Manager, Corrosion & Sustainable Infrastructure Laboratory, Western Transportation Institute, Montana State Univ., P.O. Box 174250, Bozeman, MT 59717-4250 (corresponding author). E-mail: xianming_s@coe.montana.edu

Note. This manuscript was submitted on November 19, 2010; approved on October 6, 2011; published online on October 8, 2011. Discussion period open until September 1, 2012; separate discussions must be submitted for individual papers. This paper is part of the ***Journal of Materials in Civil Engineering***, Vol. 24, No. 4, April 1, 2012. ©ASCE, ISSN 0899-1561/2012/4-381–390/$25.00.

assessment is depicted for reinforced concrete, the methodology for which can be used as a valuable tool for structural engineers and asset managers to estimate the appropriate timing of concrete maintenance and rehabilitation.

Methodology

Provided that the chloride-induced material degradation is the major durability issue, the total service life of concrete structures (denoted by t_s) can be described as (Tutti 1982; Konecny et al. 2007)

$$t_s = t_i + t_p \tag{1}$$

where t_i = period within which a sufficient amount of chlorides can accumulate on rebar surface; and t_p = time for rebar corrosion to reach an unacceptable condition. Reinforced concrete structures in the field may not be fully saturated during their service life and mechanisms other than diffusion (capillary suction) can contribute to chloride ingress and shorten their service life. In this work, however, we assume that the concrete is fully saturated and diffusion is the main mechanism of chloride ingress. The value t_i can thus be solely related to the penetration process in concrete cover by diffusion, and Fick's law is capable of predicting the chloride concentration evolution on rebar surface. The initiation period is mainly influenced by diffusion coefficients in ionic species, concrete cover depth, surface chloride concentrations, and critical chloride concentrations on rebar surface. Such variables are in principle stochastic, as corrosion damage is highly dependent on environmental parameters. Thus, the service life is a range of distribution rather than a single value. The degradation process, in which rebar experiences active corrosion, is complex and strongly depends on external conditions such as temperature and humidity. However, t_p is generally accepted to be around 4–6 years for "black bar" or uncoated mild steel bar (Bentur et al. 1997). Such a short duration can be neglected for service life modeling, compared with the relative long time frame of corrosion initiation (~100 years). In what follows, the mathematical model to be used for service life prediction is based on the conservation laws with fundamental model parameters related to the concrete characteristics and the environment to which the system is subject, which can reflect the stochastic nature and thus can account for the variability of input parameters to predict the time for deterioration and first repair. In addition, unlike the traditional treatment where only chloride diffusion is taken into consideration, the physical and chemical interactions among ionic species and cement phases are fully explored in this study.

Model for Multi-Species Transport (Method A)

From the modeling perspective, concrete structures can be divided into two physical domains, i.e., aggregate and cement paste. Aggregate is a dense and hard reinforcing component in the concrete matrix in which the diffusivities of ionic species are negligible, while the pore system in cement paste provides a zigzag diffusion path through which ionic species can migrate. Depending on the mix design of the concrete (e.g., cement type, mineral admixtures, and chemical admixtures), multiple ionic species can be present in pore solutions, among which Na^+, K^+, Ca^{2+}, Cl^-, and OH^- are most frequently encountered. Chloride ions in concrete are either free or bound. The free ones are water-soluble and can attack the passive film on the rebar surface to initiate pitting corrosion, whereas the bound ones exist in the form of chloride-aluminates, making them unavailable for free transport. In most of the traditional service life predictions of concrete structures, only chloride anions (Cl^-) are taken into consideration during the diffusion process. Although this treatment is simple and can be successfully applied to various scenarios, it fails to elucidate material degradation due to ionic and mineral interactions. There is thus a necessity to incorporate all the ionic species present in the system and reformulate the model methodology to reflect the real scenario.

To describe the ionic transport in a porous system, the technique of homogenization is indispensable, which is rooted at the microscopic scale with the subsequent integration over a representative elementary volume (Wang et al. 2001):

$$p\frac{\partial C_i}{\partial t} + (1-p)\frac{\partial S_i}{\partial t} + \nabla \cdot (pJ_i) = 0 \tag{2}$$

where C_i and S_i = free and bound concentrations of species i, respectively; p = porosity; t = time; and J_i = the flux of species i. The flux of each species in the pore solution can be given by (Hassanein et al. 1998)

$$J_i = -D_i\nabla C_i - \frac{D_i}{RT}C_iFZ_i\nabla\phi \tag{3}$$

where D_i and Z_i = diffusion coefficient and valence number for species i, respectively; F = Faraday's constant; R = gas constant; T = temperature; and ϕ = electric potential.

From the practical point of view, only chloride binding is considered in this work, which is assumed to follow the Langmuir isotherm as follows (Lu et al. 2002):

$$S_{Cl} = \frac{\alpha C_{Cl}}{1+\beta C_{Cl}} \tag{4}$$

where α and β are the binding parameters to be evaluated from measured free and bound chloride concentrations. The chloride binding effect is accounted for by combining Eqs. (4) and (6).

In the absence of externally applied electric field, the electroneutrality principle applied to the concrete pore solution, i.e., the net charge of ions in the solution should be zero. At typical concentrations, the influence of nonideality of electrolytic solution on the ionic fluxes is negligible, which indicates that the chemical activity of each species can be approximated by its corresponding concentration. Under an internally induced electric field, all the ionic species in the pore solution contribute to the electroneutrality condition. Since the electric current in an electrolyte results from the movement of charged particles, the current density can be formulated as the fluxes of all the species as follows (Hassanein et al. 1998):

$$i = pF\sum_{i=1}^{n} Z_i\left(-D_i\nabla C_i - \frac{Z_iFD_i}{RT}C_i\nabla\phi\right) \tag{5}$$

With the zero-flux boundary condition, the electroneutrality condition can be formulated as (Hassanein et al. 1998)

$$\nabla \cdot i = 0 \tag{6}$$

which serves as a supplemental equation to correlate the electric interaction among various species.

The concentrations of ionic species and the internal electric field constitute the degrees of freedom in the model with which to describe the mass transfer and local reaction. The model is accomplished by dividing the computation into two stages for each time step. The first stage is to investigate the transport of ionic species alone, with the chemical interaction being ignored. The second

J. Mater. Civ. Eng., 2012, 24(4): 381-390

stage is to check the local solubility constraint so that a certain amount of calcium carbonate can precipitate from pore solution and locally alter the pore fraction. Such two stages constitute a numeric time step during modeling, where the temporal scale should be set as small as possible to approach real and spontaneous local equilibrium.

Model for Single-Species Transport (Method B)

Based on the measured materials properties, the service life prediction can be obtained using a reliability analysis with only chloride species. Assuming chloride diffusion is the only physical process under consideration, the chloride content in concrete can be described by (Gjrv and Vennesland 1979; Buenfeld et al. 1998)

$$\frac{\partial C_{Cl}}{\partial t} = D\frac{\partial^2 C_{Cl}}{\partial x^2} \tag{7}$$

where C_{Cl} = chloride content in kg/m^3; D = chloride diffusion coefficient; x = depth from the concrete surface; and t = time. When the surface chloride concentration is a constant and the diffusion problem is described for a one-dimensional finite depth, the analytical solution for Eq. (7) can take the following form (Gjrv and Vennesland 1979):

$$C_{Cl} = C_0\left[1 - erf\left(\frac{x}{2\sqrt{Dt}}\right)\right] \tag{8}$$

where C_0 = surface chloride concentration; and erf = error function. When calculating the service of concrete concretes, C_{Cl} is treated as the corrosion initiation concentration. With given values of C_{Cl}, C_0, D, and x based on their own statistical distribution, the time for corrosion initiation can be conveniently evaluated.

Input Parameters

As domain or boundary parameters, surface concentrations, concrete cover depth, diffusion coefficients, and chloride threshold values are random variables that have a stochastic nature. Once such model parameters have been identified either from lab measurement or field practice, a random number generator based on normal, triangle, and gamma distributions to sample such stochastic values will be utilized, which can be linked with finite-element analysis to retrieve information on the time for repair and rehabilitation. In order to reflect this peculiarity, a solution to Eqs. (2)–(6) should be sampled extensively so as to reflect the probabilistic nature of the input variables. The number of samplings is a compromise between the time for the simulation and the acceptability of the simulation results. As the number of samplings increases, the confidence interval for predicted service life becomes less sensitive with respect to the stochastic nature of the input variables. The precision of the predictions can thus represent the range of service life. To this end, the simulation for the computational studies in this work is performed 10,000 times for each scenario. Based on the results of such trials, the 95% confidence intervals for the predicted time to repair and rehabilitation are evaluated.

The surface chloride concentration is an important parameter for characterizing the driving force for chloride diffusion, the value of which depends on geographic locations and structure types. In order to estimate service life in extreme conditions, various surface chloride concentrations (from 2 to 8 kg/m^3) are utilized. As the surface chloride concentrations vary with temperature, local humidity, and season alternation, a normal distribution is adopted in the simulation, as follows:

$$f(x) = \frac{1}{\sqrt{2\pi\sigma^2}}e^{[-(x-\mu)^2/2\sigma]} \tag{9}$$

where σ and μ = mean and standard deviation, respectively. The mean values for chlorides are set to 2, 4, 6 and 8 kg/m^3, with a standard deviation of 0.2 kg/m^3 for all the cases investigated. Such a standard deviation is also applied for other ionic concentrations involved in the simulation. The spectrum distributions for various chloride concentrations are presented in Fig. 1.

Diffusion coefficients of chloride and other species are highly dependent on materials characteristics and environments. In order to reflect the stochastic nature of diffusion coefficients in concrete structures, the diffusion coefficients are assumed to follow the gamma distribution given by

$$f(x\ :\ k,\theta) = x^{k-1}\frac{e^{-x/\theta}}{\theta^k\Gamma(k)} \tag{10}$$

where $x > 0$ and k, $\theta > 0$; $k = 27.05$ and $\theta = 1.42$ for chloride diffusion in concrete, respectively. A graphical representation of the chloride diffusion coefficient distribution is provided in Fig. 2,

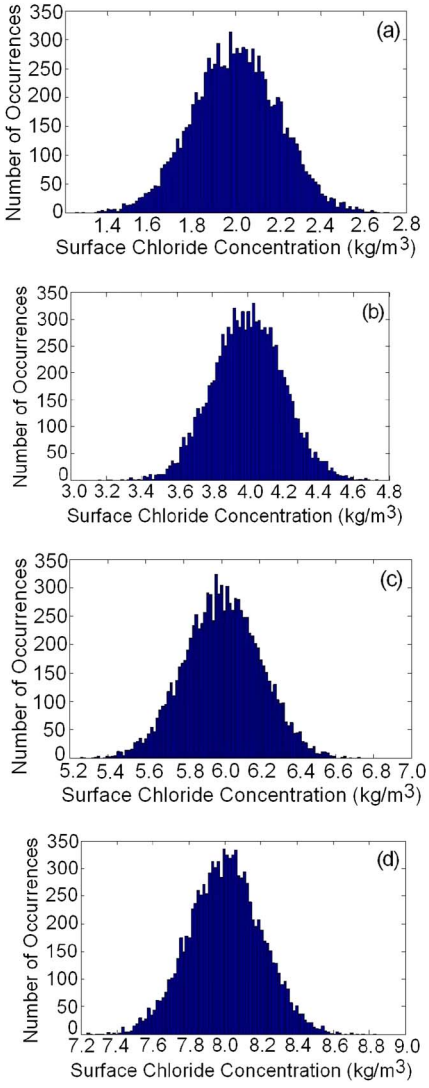

Fig. 1. Surface chloride concentration distribution according to the normal distribution: (a) 2 kg/m^3; (b) 4 kg/m^3; (c) 6 kg/m^3; (d) 8 kg/m^3

J. Mater. Civ. Eng., 2012, 24(4): 381-390

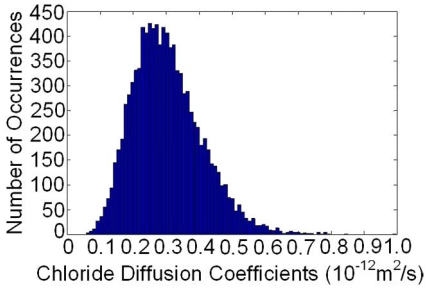

Fig. 2. Chloride diffusion coefficient distribution according to the gamma distribution

the tendency of which is also applied for other diffusion coefficients and mix designs.

The actual chloride threshold in concrete is dependent on various parameters such as cement type, composition, moisture content, and temperature. The triangular distribution is a continuous distribution with lower limit a, mode c, and upper limit b, mathematically expressed as

$$f(x,a,b,c) = \begin{cases} \dfrac{2(x-a)}{(b-a)(c-a)} & \text{for } a \le x \le c \\ \dfrac{2(b-x)}{(b-a)(c-a)} & \text{for } c \le x \le b \\ 0 & \text{otherwise} \end{cases} \quad (11)$$

In this work, the chloride threshold value is assumed to follow the symmetric triangular distribution, the shape of which is weighted toward to the center of a range of values. Based on previous studies (Hussain et al. 1995, 1996; Thomas 1996; Ann and Song 2007), the upper limit of the chloride threshold is set as 5 kg/m^3, while the lower limit remains at 0.6 kg/m^3, as illustrated in Fig. 3. Concrete cover depths in infrastructure feature natural variability, the change of which was found to follow the normal distribution from a survey on bridge decks in Virginia (Kirkpatrick et al. 2003). For all the concrete cover depth utilized in this work, a standard deviation of 5 mm is assumed; the probability for the thickness distribution is shown in Fig. 4 for concrete cover depths with a mean value of 50 mm.

Experimental

In order to cover a wide range of design configurations, 14 concrete mix designs were considered, the details of which can be found in Table 1. A water-to-cementitious-materials (w/cm) ratio of 0.40 was specified for all the mix designs. An ASTM specification

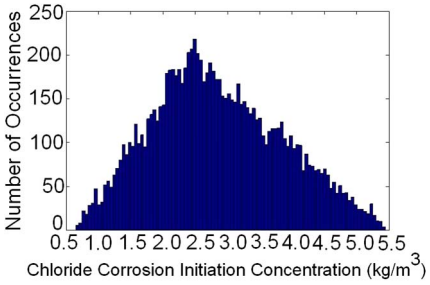

Fig. 3. Chloride corrosion initiation concentration distribution according to the triangular distribution

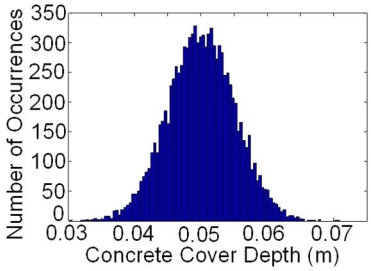

Fig. 4. Concrete cover depth distribution according to the normal distribution

C150-07 Type I/II low-alkali Portland cement from the Ash Grove Montana City Plant (Clancy, MT) was used. Coarse aggregates (with maximum size of 3/400 or 19 mm) and fine aggregates (clean, natural silica sand) were purchased from the JTL Group (Belgrade, MT). Glenium 3030 and Micro-Air were used as the ASTM C 494 Type A/F water reducing agent and the ASTM C 260 air-entraining agent, respectively, and at the dosage per the instructions. For each concrete mix, at least three replicate 12″ by 6″ (diameter 305 mm × height 152 mm) cylinders were prepared. The coarse aggregates and fine aggregates were oven-dried and then potable water was added in the amount twice as much as their absorption capacity (e.g., 1.8%). The aggregates were then soaked for 24 h to ensure that they had fully absorbed moisture and had moisture in excess of the surface-saturated-dry (SSD) condition. The saturated aggregates and the excessive water were used in the mix, taking into account the excessive water when calculating the w/cm ratio. The fine and coarse aggregates were added to the 2-cubic-feet (57-L) mixer and mixed until a homogeneous mixture was obtained. Then the cement was added and mixed again until a homogeneous mixture was obtained. Next, water was added from a graduated cylinder and mixed until the concrete is homogeneous and of the desired consistency. The batch was remixed periodically during the casting of the test specimens and the mix container was covered to prevent evaporation. Slump and air content measurements were performed by the ASTM C 143 and C 173 methods, respectively, to check the workability and quality of the freshly mixed concrete. Fresh concrete was cast into hollow poly(vinyl chloride) piping cylinders and then carefully compacted to minimize the amount of entrapped air. The cylindrical samples were demolded after curing for 24 h with over 90% relative humidity. After demolding, the samples were cured in the moist cure room (with over 90% relative humidity) for another 359 days before the accelerated chloride migration test.

In addition, nine mortar mixes (mixes 1, 3, 5, 7, 9, 11, 13, 15, and 17 in Table 1) were prepared without any coarse aggregates, water-reducer, or air-entraining agent. The w/cm ratio of the mortar samples was set at 0.45 instead of 0.40, in light of workability concerns. For each mix design, at least three replicate 2″ by 4″ (diameter 51 mm × length 102 mm) cylinders for diffusivity testing were prepared. This aims to shed light on the role of coarse aggregates and to better interpret the chloride diffusion data in concrete containing various types and amounts of mineral admixtures. For mortar samples, cement is mixed with water using a low-speed hand mixer for 5 min. Subsequently, fine aggregates, with a maximum size of 1.18 mm in diameter, were added, after which the slurries were stirred for 3 min. The fine aggregates were prepared to SSD condition in advance. All the slurries were cast into hollow poly(vinyl chloride) piping cylinders and then carefully compacted to minimize the amount of entrapped air. The cylindrical samples were demolded after curing for 24 h with over 90% relative humidity. After demolding, the samples were cured with over 90%

J. Mater. Civ. Eng., 2012, 24(4): 381-390

Table 1. Mix Design Parameters and the Properties of Concrete Samples Containing Various Types and Amounts of Mineral Admixtures

Ingredients	Mix number																	
	1	2	3	4	7	8	9	10	11	12	13	14	15	16	17	18		
Portland cement (lb)	75	75	56	56	56	56	56	56	68	68	68	68	68	68	38	38		
Fly ash (class F) (lb)			19	19	15	15	15	15										
Silica fume (lb)					4	4			8	8								
Metakaolin (lb)							4	4			8	8						
Ultra fine fly Ash (lb)													8	8				
Blast furnace slag (lb)															38	38		
Micro-Air (ml)		22		33		33		33		22		22		21		22		
Glenium 3030 (ml)	150	165	33	24	133	44	200	133	266	238	255	238	150	150	155	166		
Water (lb)	28	25	28	28	24	26	25	24	28	28	28	28	25	25	27	27		
Fine aggregate (lb)	106.1	129.5	139.3	127.3	139.1	127.2	139.4	127.5	140.3	128.4	140.9	129.0	140.7	128.8	140.4	128.5		
Moisture content (%)	3.6	3.6	3.6	3.6	3.6	3.6	3.6	3.6	3.6	3.6	3.6	3.6	3.6	3.6	3.6	3.6		
Course aggregate (lb)	162.4	199.3	210.3	192.8	214.5	194	213.5	196.4	211.8	194	212.8	195.1	216.2	197.9	213	195.1		
Moisture content (%)	0.55	2.106	0.667	0.96	2.769	1.66	2.089	2.708	0.647	0.712	0.718	0.886	2.397	2.43	1.133	1.248		
Slump (in)	2.5	3	2.5	3.5	3	4	4.5	3.5	2.25	2	4	3.5	4	4	2	5.25		
Entrained air (%)	2.5	6.5	2.5	5.5	3.75	5.6	2.75	6.5	2.25	5.75	2.5	6	1.75	7	2.5	6		
Volume (ft^3)	3	3	3	3	3	3	3	3	3	3	3	3	3	3	3	3		
Strength at 90 days (psi)	10,367	7,834	9,404	5,654	10,020	5,841	9,557	6,833	9,848	7,869	11,623	7,070	10,335	6,476	8,560	5,544		

relative humidity for another 89 days before the accelerated chloride migration test.

The chloride diffusion coefficients of 90-day mortar samples and 360-day concrete samples were measured using an accelerated chloride migration test detailed elsewhere (Yang et al. 2009; Shi et al. 2011). The testing procedures of chloride binding capacity of mortar are detailed in the reference (Barneyback 1981). Diffusion coefficients other than chlorides were taken from the work of Wang et al. (2001). This work pertains to the concrete reinforced with black bar, instead of epoxy-coated rebar or corrosion-resistant rebar.

Results and Discussion

Effect of Mix Design on Service Life

Chloride diffusion in concrete materials strongly depends on the environment, as such species will either chemically or physically interact with cement phases. Chloride transport through concrete materials will thus be eventually influenced by the pore structure, the physical or chemical binding, and the inclusion of supplementary cementitious materials or chemical admixtures. Using the proposed two methods, transport of chloride ions in various mix designs was simulated, the results of which are presented in Table 2.

All concrete mixes investigated had a 50%-probability service life of 114 years or longer (with a surface chloride concentration of 6 $kg/m^3$and concrete cover of 50 mm), which highlights the great potential of reinforced concrete as a construction material when the concrete is made using the best practices of construction and curing and is free of cracking. The data in Table 2 also suggest that when the concrete is made using the best practices, partially replacing cement with class *F* fly ash, silica fume, metakaolin, or blast furnace slag tends to decrease the service life of reinforced concrete or at least show little benefits to its service life. This trend contradicts what has been generally reported in published literature and is likely attributable to the fact that the concrete made without any mineral admixtures (mixes 1 and 2) featured unusually low chloride diffusion coefficients on the order of 10^{-13} m^2/s. While the chloride diffusion coefficients did not differ greatly among the concrete mixes investigated, the predicted service life of reinforced concrete showed a certain degree of variations. Finally, for all these high-quality concrete mixes, the effects of air entrainment on the chloride diffusivity in concrete and the service life of reinforced concrete were not dramatic and did not show a clear trend. As mentioned previously, the rate of chloride migration depends not only on the diffusion rate of chloride ions but also the on chloride binding capability of concrete materials. It is evident from Table 2 that for the 10, 50, and 90% likelihood of corrosion initiation, the service life predicted from multispecies model (method A) is generally longer than that obtained from single-species model (method B), which is due to the incorporation of chloride binding in the former case.

Effect of Surface Chloride Concentration on Service Life

Concrete structures located in different regions are exposed to varying degrees of corrosivity (e.g., various levels of chlorides), as the amount and frequency of salt usage in Northern snow states vary significantly and the attack from marine environments in coastal states differs geographically. Such variations are reflected on the surface chloride concentrations for chlorides to migrate into concrete structures. The chloride concentrations on concrete surface

J. Mater. Civ. Eng., 2012, 24(4): 381-390

Table 2. Predicted Service Life for Various Mix Designs

Mix design	D_{Cl} (10^{-13} m^2/s)	Chloride binding parameters α and β (L/mg)	Service life from method A[a] (year)(10, 50, and 90%)	Service life from method B[a] (year)(10, 50, and 90%)
1	2.50	3.61×10^{-3}; 5.35×10^{-5}	103;285;624	95;182;521
2	2.74	3.61×10^{-3}; 5.35×10^{-5}	91;179;584	79;168;523
3	2.36	2.12×10^{-3}; 2.29×10^{-5}	102;174;628	87;157;593
4	3.77	2.12×10^{-3}; 2.29×10^{-5}	64;136;348	53;121;326
7	2.99	1.25×10^{-3}; 3.63×10^{-5}	79;114;405	65;107;384
8	3.25	1.25×10^{-3}; 3.63×10^{-5}	83;159;481	77;143;438
9	3.27	1.25×10^{-3}; 1.77×10^{-5}	94;168;498	83;152;467
10	3.14	1.25×10^{-3}; 1.77×10^{-5}	83;171;458	73;148;412
11	3.80	2.18×10^{-3}; 4.12×10^{-5}	62;157;371	53;135;348
13	2.90	1.58×10^{-3}; 2.21×10^{-5}	71;184;532	67;167;481
14	3.7	1.58×10^{-3}; 2.21×10^{-5}	62;148;397	53;136;356
15	3.71	2.95×10^{-3}; 3.75×10^{-5}	59;163;328	52;151;305
17	3.52	2.16×10^{-3}; 4.08×10^{-5}	53;167;324	48;145;296
18	2.35	2.16×10^{-3}; 4.08×10^{-5}	116;237;603	97;193;541

Note: Surface chloride concentration is maintained at 6 kg/m^3 and concrete cover depth is 50 mm.
[a]A and B denote the multispecies transport model and the single-species transport model, respectively.

serve as the driving force for chloride ingress, thus showing a significant effect on the service life of concrete. To investigate the effect of surface chloride concentration on the service life of reinforced concrete, numerical predictions are conducted with four levels of surface chloride concentrations, i.e., 2, 4, 6, and 8 kg/m^3, respectively. A concrete cover depth measuring 50 mm in thickness is laid over the rebar surface for all the cases studied, after which the computational investigation is conducted to explore the long-term protection. The initial conditions for concentrations of Na^+, K^+, Ca^{2+}, and OH^- within the concrete domain are 2, 2, 3, and 7 kg/m^3, respectively, and the boundary conditions for such species also remain at those values. To determine whether the chloride threshold concentration for active corrosion has been reached on rebar surface, the chloride content on rebar surface is monitored against time, and a randomly generated chloride threshold value is used as a reference to identify the service life. Based on the evolution of such curves against time, the value of t_i is determined, which is considered to be the time needed to initiate active corrosion of rebar. The current treatment incorporates the influence of mutual interaction between chloride and hydroxyl ions on chloride threshold values.

The effect of surface chloride concentration is explored by comparing the predicted service life spectrum for four scenarios, indicated in Fig. 5. However, the surface chloride concentration and the chloride threshold value are random numbers. Based on the modeling results, chloride inward-diffusion with the lowest surface chloride concentration is the most sluggish process. With the surface chloride concentration increasing, the service life decreases significantly. For the case in which the surface chloride concentration of mix design 1 remains at 6 kg/m^3, the 90% likelihood of corrosion initiation is around 600 years. The preceding discussion is based on the assumption that concrete is fully saturated with water. However, alternate wetting and drying cycles can change the chloride content on concrete surface. For a concrete cover with a depth of 50 mm, the time for chlorides to arrive at the chloride threshold level is from 150 to 600 years under various exposure conditions in Fig. 5. It is obvious that with the current concrete cover depth used by highway agencies (at least 3″ or 76 mm for chloride-laden environments), it is likely to obtain a reliable protection against chloride attack, where the chloride concentrations on rebar surface can be well below the critical threshold value for corrosion initiation even after 100 years.

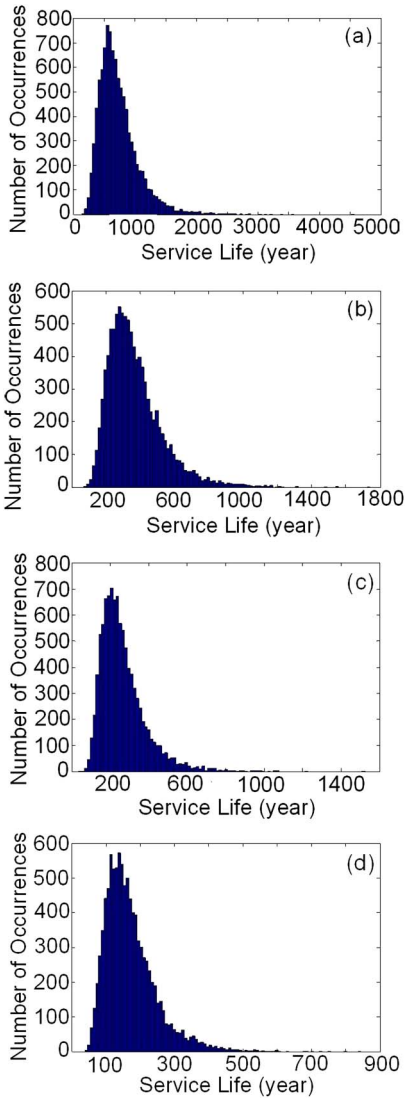

Fig. 5. Predicted surface life for concrete structures with surface chloride concentrations: (a) 2 kg/m^3; (b) 4 kg/m^3; (c) 6 kg/m^3; (d) 8 kg/m^3

J. Mater. Civ. Eng., 2012, 24(4): 381-390

Effect of Cracking Level on Service Life

Concrete structures are subject to environmental loadings (e.g., freeze/thaw cycles) and periodic traffic load under normal service conditions, leading to cracks characterized by various densities. Poor practices during construction and curing can also lead to the initiation and propagation of cracks in concrete. The effect of crack density has practical implication for the durability, reliability, and serviceability of concrete. Chloride transport through cracks over a long period of time is of primary concern for performance evaluation. Durability of concrete infrastructure is significantly affected by the presence of cracks, as they can facilitate the chloride ingress by acting as preferential channels. This consensus has been widely accepted, but a quantitative description is still lacking. Francois et al. (1998) conducted a corrosion study by exposing loaded reinforced concrete beams to salt fog for twelve years. They found that the tensile microcracking in concrete as a result of service loading was responsible for accelerating chloride penetration, whereas the existence and width of microcracks (with width less than 0.5 mm) did not influence the development of the rebar corrosion.

The simulation domains are established in Fig. 6 to investigate the effects of crack on service life, where four levels of crack configurations are presented, i.e., 50, 80, 145, and 207 m^{-1}, respectively. Here, the crack density is defined as the total crack length per unit area. The initial conditions for Na^+, K^+, Ca^{2+}, and OH^- are chosen as 2, 2, 3, and 2 kg/m^3 respectively, with the boundary conditions for such species having the same values. The surface chloride concentration remains at 5 kg/m^3 and the multispecies model is utilized. Diffusion coefficients for ionic species in cracks are taken from the work of Li and Gregory (1974).

The effect of crack density on service life is evaluated by comparing the predicted chloride concentration profiles on rebar surface. Due to the presence of cracks in the two-dimensional domains, the distribution of chlorides on rebar surface is not uniform. Based on the modeling results, average chloride concentrations on rebar surface are utilized as the indicator, i.e., the chloride surface concentration after the introduction of cracks is determined by integration of the chloride concentration across the rebar surface and then divided by the rebar surface area. The time to corrosion initiation is presented in Fig. 7, where the model outputs as a function of crack density are given. As shown in Fig. 7, the service life of reinforced concrete decreases as the cracking level of concrete increases. These cracks simulated in the FEM model were at least 0.5 mm in width. The actual diffusion path traveled by ionic species in a cracked concrete is shorter than in a crack-free solid. For the case in which the crack fraction is low, the short circuit path is far apart. Upon increasing of crack density, the distance for chloride ingress among various diffusion channels decreases. Based on the modeling results, chloride diffusion in crack-free concrete is the slowest process. With the crack density increasing, more chlorides are accumulating around rebar surface. When the crack density exceeds 200 m^{-2}, the service life shows no significant dependence on further increase in crack density, which is attributable to the forming of continuous netlike configuration in the concrete domain.

Effect of Coarse Aggregate on Service Life

From the practical point of view, concrete can be treated as a structure having two constituents: cement paste and aggregates. Aggregates are a dense phase that is randomly distributed within

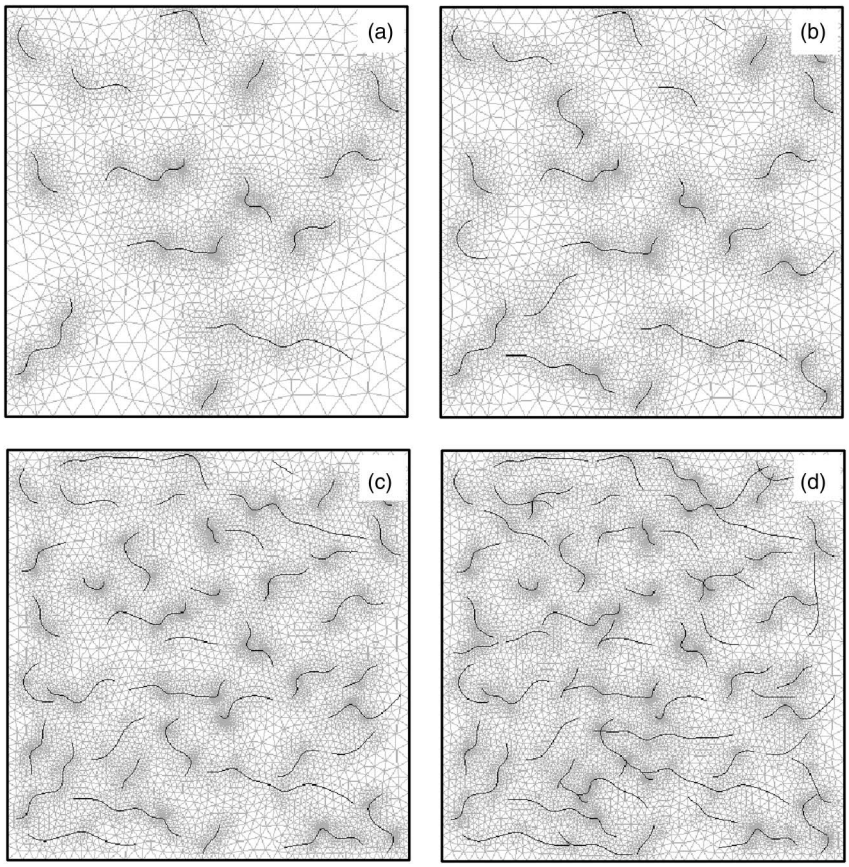

Fig. 6. Crack configurations with various densities for service life prediction: (a) 50 m^{-1}; (b) 80 m^{-1}; (c) 145 m^{-1}; (d) 207 m^{-1}

J. Mater. Civ. Eng., 2012, 24(4): 381-390

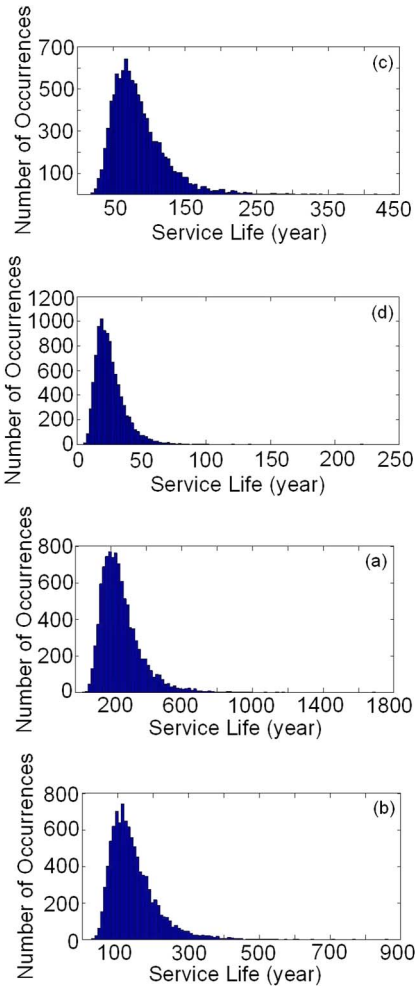

Fig. 7. Effect of crack densities on service life prediction: (a) 50 m^{-1}; (b) 80 m^{-1}; (c) 145 m^{-1} ; (d) 207 m^{-1}

continuous cement matrix. When concrete is water-saturated, the pores in cement matrix form a continuous channel system, within which chlorides diffuse and transport toward rebar surface. The diffusivity of ionic species in aggregates is very small, which leads to appreciable heterogeneities of chloride diffusion within concrete.

Traditionally, concrete is considered to have a heterogeneous interfacial transition zone (ITZ) with about 30 μm of porosity gradient on the surface of each coarse aggregate, featuring a highly localized w/cm ratio and high porosity relative to the cement paste phase (Diamond and Huang 2001; Scrivener et al. 2004). This, however, is debatable since "the higher porosity present initially is significantly diminished by the migration of ions during hydration" (Ollivier et al. 1995) and "the extra space produced by the wall effect is filled in by CH deposits" (Alexander et al. 1999). It is believed that it is possible to eliminate the presence of ITZ through best practices of construction and curing, such as the use of SSD aggregates and high-speed stirring during mixing of fresh concrete.

If we ignore the presence of paste-aggregate ITZ, the diffusion coefficients in paste and mortar can be combined with the amount of aggregates to predict transport properties of concrete. To gain an acceptable description for chloride diffusion in concrete structures, the mean field theory is adopted to evaluate the effective diffusion coefficients, where a two-dimensional simulation domain with the same size as mentioned previously is utilized. To gain a phenomenological description of chloride diffusion in hetero-structural concrete, the effective diffusion coefficient for a two-phased structure can be described by (Zeng 2007)

$$D_{eff} = D_c \frac{\mathrm{D_a} + \mathrm{K_a D_c} + \mathrm{K_a}\phi(\mathrm{D_a} - D_c)}{D_a + K_a D_c - \phi(D_a - D_c)} \tag{12}$$

where D_c stands for the chloride diffusion coefficients in cement past, while D_a is that for aggregates, and ϕ and K_a are the volume fraction and the shape factor for the aggregates, respectively. For spherical aggregates, $K_a = 2$. Eq. (12) is utilized in this work to extrapolate diffusion coefficients with various aggregate fractions from the measured chloride diffusion coefficients in concrete samples.

For the simulation, a rectangular domain dimensioned by 50×50 mm is taken from a semi-infinite concrete with its left surface exposed to chloride-containing solution. The multispecies model is utilized. Four volume fractions of aggregate are used, i.e., 0.2, 0.4, 0.6, and 0.8. For convenience, the diffusion coefficients of ionic species in aggregate are set to zero. Four kinds of concrete mix designs are utilized for simulation, and the cumulative percentage of corroded structures for different aggregate volume fraction are shown in Fig. 8. All the curves share the same pattern across the entire temporal domain. The large difference in diffusion rate between aggregates and cement paste complicates the service life prediction of concrete. For concrete structures with aggregates, the chloride diffusion rate was found to be quite different from that in the corresponding homogeneous medium. The overall flux decreases as the volume fraction of aggregates increases. The same behavior is also observed for other aggregate fractions but shifted with respect to time and positions.

Effect of Concrete Cover Depth on Service Life

Concrete cover serves as a physical barrier to retard the ingress of deleterious species. Usually, an increase in the thickness of the concrete cover lead to beneficial effects, because it increases the barrier to the various aggressive species moving toward the reinforcement and increases the time for corrosion to initiate. In reality, however, the cover thickness cannot exceed certain limits, for mechanical and practical reasons (Francois et al. 1998).

To ensure the durability of concrete structures for a specific service life, concrete cover depths need to be evaluated with a theoretical method. According to the numerical method for multispecies diffusion, the relation between service life and concrete cover depth is predicted, the results of which are shown in Fig. 9. Such profiles provide qualitative information to predict service life against concrete cover depth. As the model incorporates probability distribution of input variables, the predictions can be used not only for a particular structure but also for a large population of bridges.

As shown in Fig. 9, for the mineral concrete mixes investigated, as the concrete cover depth increases, the time to corrosion initiation of rebar is predicted to increase exponentially, highlighting the importance of cover depth in extending the service life of reinforced concrete exposed to external chlorides. According to the model calculations, it would take more than 100 years for the chloride ions in an aggressive environment (with surface chloride content of 8 kg/m^3) to reach the threshold level at a depth of 60 mm. It should be cautioned that the chloride diffusivity data used for the model were measured using specimens cored from the center of a large concrete sample. In field construction, the top layer of the concrete cover is likely to have much higher chloride diffusivity than the interior of the concrete, in light of the possible defects derived from bleeding and water evaporation at the top layer. Furthermore, the field construction is unlikely to achieve the same level of detailed quality assurance as implemented in

J. Mater. Civ. Eng., 2012, 24(4): 381-390

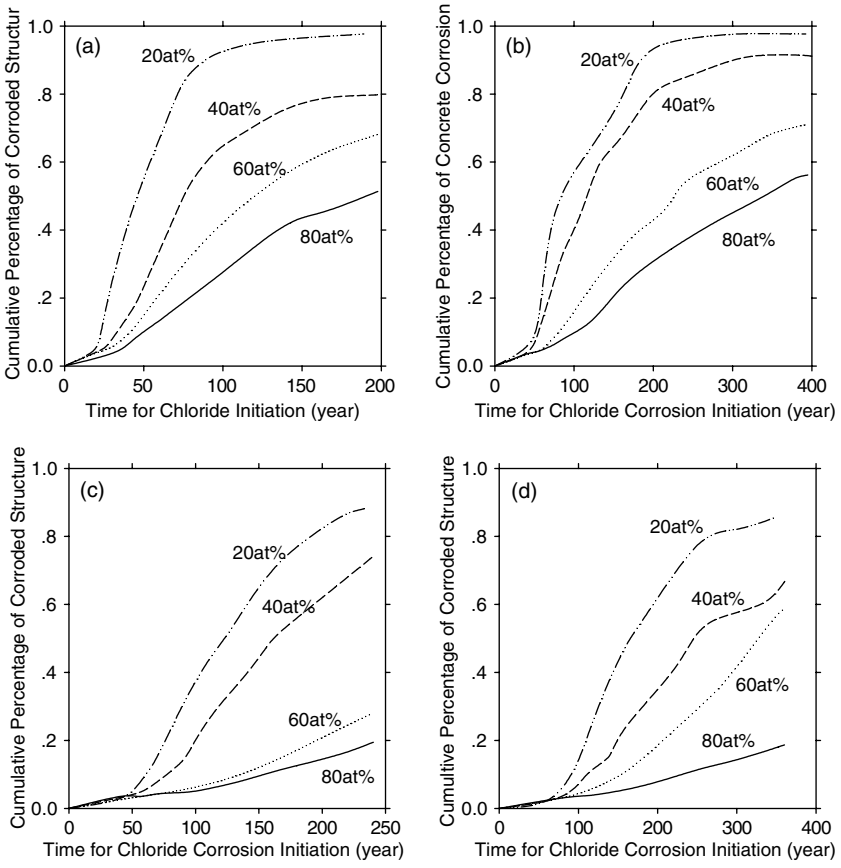

Fig. 8. Effect of aggregate fraction on chloride-induced corrosion: (a) mix design 2; (b) mix design 4; (c) mix design 8; (d) mix design 11

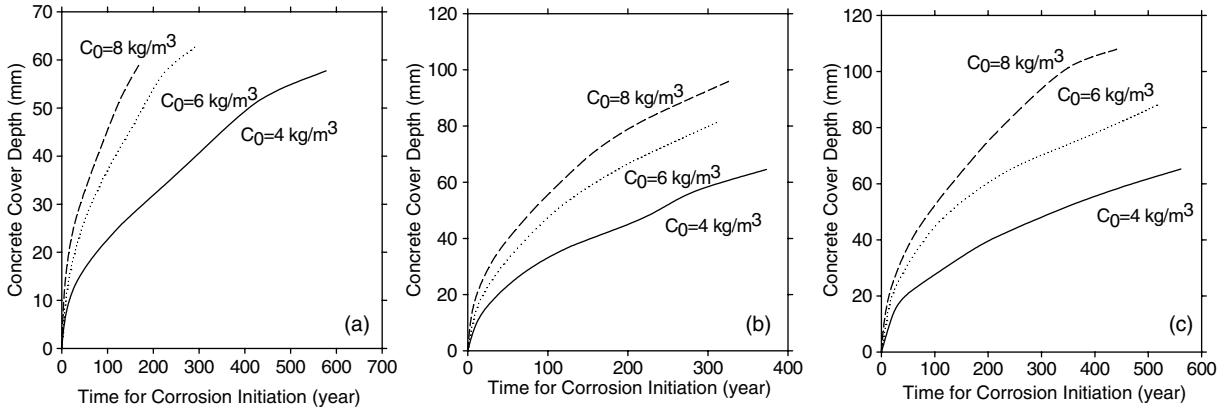

Fig. 9. Variation of service life with respect to concrete cover depth: (a) mix design 2; (b) mix design 4; (c) mix design 8

the laboratory study and cracking cannot be fully eliminated for the service life prediction considerations. In this context, a thicker-than-predicted concrete cover is needed for the target service life of concrete structures in the field environment and the importance of good construction and curing practices cannot be overemphasized.

Concluding Remarks

A two-dimensional FEM model, coupled with the stochastic technique, is developed to study the service life of concrete structures under various conditions. In order to provide a reliable and statistical method to predict service life of concrete structures, concrete cover depth, chloride diffusion coefficients, surface chloride concentration, cracks and aggregates are taken into consideration, which are stochastically sampled. Starting from the equation of mass balance, the model incorporates the effect of various internal and external factors, and then explores the important features of ionic transport in concrete. The technique proposed in this work (e.g., multispecies transport model) may prove to be very effective in predicting chloride migration and generating statistical conclusions about the service life of concrete, which allows the civil engineers to estimate the rate of chloride ingress and speculate the deterioration risk of reinforced concrete.

J. Mater. Civ. Eng., 2012, 24(4): 381-390

Future improvements could be made to the model so that it takes into account the time-dependency of transport properties of concrete, the repair or replacement of concrete cover, the corrosion propagation, the chloride penetration mechanisms other than diffusion (e.g., wicking), the structure geometry, the environmental humidity and temperature fluctuations and the decay of structures under coupled physical, chemical, and mechanical deterioration processes etc. With continued improvements on such models, they could also be used for life cycle costing and for the timing of repair or rehabilitation strategies.

Acknowledgments

The authors acknowledge the financial support provided by the California Department of Transportation as well as the Research & Innovative Technology Administration (RITA) at the U.S. Department of Transportation for this project. The authors are indebted to the Caltrans Research Manager Peter S. Lee and the technical panel consisting of Rob Reis, Doug Parks, Rudy Lopez, and Charlie Sparkman, for their continued support throughout this project. We owe our thanks to Doran Glauz and Larry McCrum at Caltrans for discussions related to the handling and preparation of the coarse and fine aggregates prior to the batching operations. We appreciate the following professionals who provided assistance to this research: Richard Sullivan (Caltrans), Richard Halverson (Headwaters Resources), Steve Beck (Western Pozzolan Co.), Jim Anderson (BASF/MB Admixtures), Ken McPhalen (Advanced Cement Technologies), Kevin Foody (Boral Material Technologies), Greg Juell (Lehigh Southwest Cement Co.), and Jeff Wiest (Ashgrove Montana City Plant). We also thank Dr. Brett Gunnink of the MSU Civil Engineering Department for coordinating the use of Bulk Materials Laboratory, Concrete Wet Curing Room, and other facilities. Finally, we owe our thanks to the following individuals at the Western Transportation Institute for providing help in various stages of the laboratory investigation: Doug Cross, Zhengxian Yang, Matthew Mooney, and Eric Schon.

References

Alexander, M. G., Arliguie, G., Ballivy, G., Bentur, A., and Marchand, J (1999). "Engineering and transport properties of the interfacial transition zone in cementitious composites." *State-of-the-Art Rep. of RILEM TC 159-ETC and 163-TPZ*, ⟨http://rilem.net/gene/main.php?base=500219&id_publication=84⟩ (Jul. 15, 2011).

Ann, K. Y., and Song, H. (2007). "Chloride threshold level for corrosion of steel in concrete." *Corros. Sci.*, 49(11), 4113–4133.

Barneyback, R. S. Jr., and Diamond, S. (1981). "Expression and analysis of pore fluids from hardened cement pastes and mortars." *Cem. Concr. Res.*, 11(2), 279–285.

Basheer, L., Kropp, J., and Cleland, D. (2001). "Assessment of the durability of concrete from its permeation properties: A review." *Constr. Build. Mater.*, 15(2–3), 93–103.

Bentur, A., Diamond, S., and Berke, N. S. (1997). *Steel corrosion in concrete*, E & FN Spon, London.

Buenfeld, N. R., Glass, G. K., Hassanein, A., M., and Zhang, J. (1998). "Chloride transport in concrete subjected to electric field." *J. Mater. Civ. Eng.*, 10(4), 220–228.

Diamond, S., and Huang, J. (2001). "The ITZ in concrete—A different view based on image analysis and SEM observations." *Cem. Concr. Compos.*, 23(2–3), 179–188.

Fasjardo, G., Escadeillas, G., and Arliguie, G. (2002). "Electrochemical chloride extraction from steel-reinforced concrete specimens contaminated by 'artificial' sea-water." *Cem. Concr. Res.*, 32(2), 323–326.

Francois, R., Arliguie, G., and Castel, A. (1998). "Influence of service cracking on service life of reinforced concrete." *Proc., 2nd Int. Conf. Concrete under Severe Conditions*, CONSEC '98, E & FN Spons, London.

Gjørv, O. E., and Vennesland, Ø. (1979). "Diffusion of chloride ions from seawater into concrete." *Cem. Concr. Res.*, 9(2), 229–238.

Glass, G. K., and Buenfeld, N. R., (1997). "The presentation of the chloride threshold level for corrosion of steel in concrete." *Corros. Sci.*, 39(5), 1001–1013.

Glass, G. K., and Buenfeld, N. R. (2000a). "Chloride-induced corrosion of steel in concrete." *Prog. Struct. Eng. Mater.*, 2(4), 448–458.

Glass, G. K., and Buenfeld, N. R. (2000b). "The influence of chloride binding on the chloride induced corrosion risk in reinforced concrete." *Corros. Sci.*, 42(2), 329–344.

Hassanein, A. M., Glass, G. K., and Buenfeld, N. R. (1998). "A mathematical model for electrochemical removal of chloride from concrete structures." *Corrosion*, 54(4), 323–332.

Hussain, S. E., Al-Gahtani, A. S., and Rasheeduzzafar (1996). "Chloride threshold for corrosion of reinforcement in concrete." *ACI Mater. J.*, 93(6), 534–538.

Hussain, S. E., Rasheeduzzafar, Al-Musallam, A., and Al-Gahtani, A. S. (1995). "Factors affecting threshold chloride for reinforcement corrosion in concrete." *Cem. Concr. Res.*, 25(7), 1543–1555.

Jiang, Q. M., Yang, L. F., and Chen, Z. (2010). "Stochastic analysis of chloride profiles in concrete structures." *Adv. Mater. Res.*, 163–167, 3364–3368.

Khatri, R. P., and Sirivivatnanon, V. (2004). "Characteristic service life for concrete exposed to marine environments." *Cem. Concr. Res.*, 34(5), 745–752.

Kirkpatrick, T. J., Weyers, R. E., Anderson-Cook, C., and Sprinkel, M. M. (2002). "Probabilistic model for the chloride-induced corrosion service life of bridge decks." *Cem. Concr. Res.*, 32(12), 1943–1960.

Kirkpatrick, T. J., Weyers, R. E., Anderson-Cook, C., Sprinkel, M. M., and Brown, M. C. (2003). "A model to predict the impact of specification changes on chloride induced corrosion service life of Virginia bridge decks." *Rep. No. VTRC03-CR4*, Virginia Transportation Research Council (VTRC), Charlottesville, VA.

Konecny, P., Tikalsky, P. J., and Tepke, D. G. (2007). "Performance evaluation of concrete bridge deck affected by chloride ingress: Simulation-based reliability assessment and finite element modeling." *Transportation Research Record 2028*, Washington, DC, 3–8.

Li, Y., and Gregory, S. (1974). "Diffusion of ions in sea water and in deep-sea sediments." *Geochim. Cosmochim. Acta*, 88, 703–714.

Lu, X., Li, C., and Zhang, H. (2002). "Relationship between the free and total chloride diffusivity in concrete." *Cem. Concr. Res.*, 32(2), 323–326.

Ollivier, J. P., Maso, J. C., and Bourdette, B. (1995). "Interfacial transition zone in concrete." *Adv. Cem. Based Mater.*, 2(1), 30–38.

Orellan, J. C., Escadeillas, G., and Arliguie, G. (2004). "Electrochemical chloride extraction: efficiency and side effects." *Cem. Concr. Res.*, 34(2), 227–234.

Scrivener, K. L., Crumbie, A. K., and Laugesen, P. (2004). "The interfacial transition zone (ITZ) between cement paste and aggregate in concrete." *Interfacial Sci.*, 12(4), 411–421.

Shi, X., Yang, Z., Liu, Y., and Cross, D. (2011). "Strength and corrosion properties of Portland cement mortar and concrete with mineral admixtures." *Constr. Build. Mater.*, 25(8), 3245–3256.

Thomas, M. (1996). "Chloride thresholds in marine concrete." *Cem. Concr. Res.*, 26(4), 513–519.

Tutti, K. (1982). "Corrosion of steel in concrete." *Rep. No. 4-82*, Swedish Cement and Concrete Research Institute, Stockholm, Sweden.

Wang, W., Li, L. Y., and Page, C. L. (2001). "A two-dimensional model of electrochemical chloride removal from concrete." *Comput. Mater. Sci.*, 20(2), 196–212.

Yang, Z., Shi, X., Creighton, A. T., and Peterson, M. M. (2009). "Effect of styrene–butadiene rubber latex on the chloride permeability and microstructure of Portland cement mortar." *Constr. Build. Mater.*, 23(6), 2283–2290.

Zeng, Y. (2007). "Modeling of chloride diffusion in hetero-structured concretes by finite element method." *Cem. Concr. Compos.*, 29(7), 559–565.